Applied Magnetic Resonance (2023) 54:47–58
https://doi.org/10.1007/s00723-022-01485-9

Applied
Magnetic Resonance

ORIGINAL PAPER

Triplet Born Radical Pairs and the Low Field Effect

Jonathan R. Woodward[1]

Received: 30 April 2022 / Revised: 31 May 2022 / Accepted: 11 July 2022 /
Published online: 6 August 2022

Abstract
The importance of photochemical reactions proceeding through the formation of spin-correlated radical pairs is becoming increasingly apparent, due to their roles in biological magnetic field sensing and optoelectronic devices. Here, we consider the spin-dynamics of triplet born radical pairs under varying weak magnetic field conditions and in doing so provide a simplified model for understanding the low field effect by identifying triplet states that cannot undergo coherent mixing to singlet states in zero magnetic field.

1 Introduction

The Radical Pair Mechanism (RPM) was developed in the 1960s [1–3] to explain the anomalous line intensities observed in electron spin resonance (ESR) [4] and Nuclear Magnetic Resonance (NMR) experiments [5–7]. The RPM suggested that reactions involving spin correlated radical pairs (RPs) should show reaction rates and yields sensitive to the application of external magnetic fields, and such behaviour was subsequently observed experimentally in the mid-1970s [8, 9]. Subsequently, an entire field known as Spin Chemistry developed, based around phenomena exhibited by RPs. The RPM has received significant attention in recent years due to its importance in potentially explaining the magnetoreception ability of many animals and its applications in photoactive solid state devices such as light emitting diodes and solar cells. With regard to the sensitivity of biological systems to very weak magnetic fields, including the geomagnetic field and environmental electromagnetic fields, a particular feature of RP behaviour, known as the low field effect (LFE) lies at the heart of the hypothesis of a RP-based interaction mechanism.

Almost all theoretical studies of RPs model the effects of magnetic fields on the time evolution of an initially singlet RP populations undergoing spin-selective

✉ Jonathan R. Woodward
jrwoodward@g.ecc.u-tokyo.ac.jp

[1] Graduate School of Arts and Sciences, The University of Tokyo, 3-8-1 Komaba, Meguro, Tokyo 153-8902, Japan

reaction to form products. Recently we have performed Liouville-state-based simulations on reactions of both singlet and triplet born RPs. These simulations reveal interesting features, some of which we present here. Examination of the fates of different spin states of triplet born RPs provides a simpler way to visualise and explain the so-called low field effect (LFE) which is believed to be responsible for biological responses to the geomagnetic field.

2 Triplet Eigenstates of Radical Pairs Under Varying Magnetic Field Conditions

In general, RPs generated in thermal processes from diamagnetic molecules are born in the singlet state, while photochemically generated RPs may be formed in an initially singlet or triplet state, depending on the photophysics of the RP precursor. Some molecules generate both singlet and triplet born RPs on photoexcitation, e.g. [10] and many molecules can generate triplet RPs with an unequal distribution of the three triplet substates, T_{+1}, T_0 and T_{-1} through the Triplet Mechanism (TM) [11]. Here, we consider only triplet born RPs with equal populations of the triplet substates (i.e. $[T_{+1}] = [T_0] = [T_{-1}]$). A common simplified model for a radical pair in zero and applied magnetic field due to the Zeeman effect is given in Fig. 1a. In this model, in zero field the S state can undergo coherent spin-state mixing with all three triplet states. However, in the presence

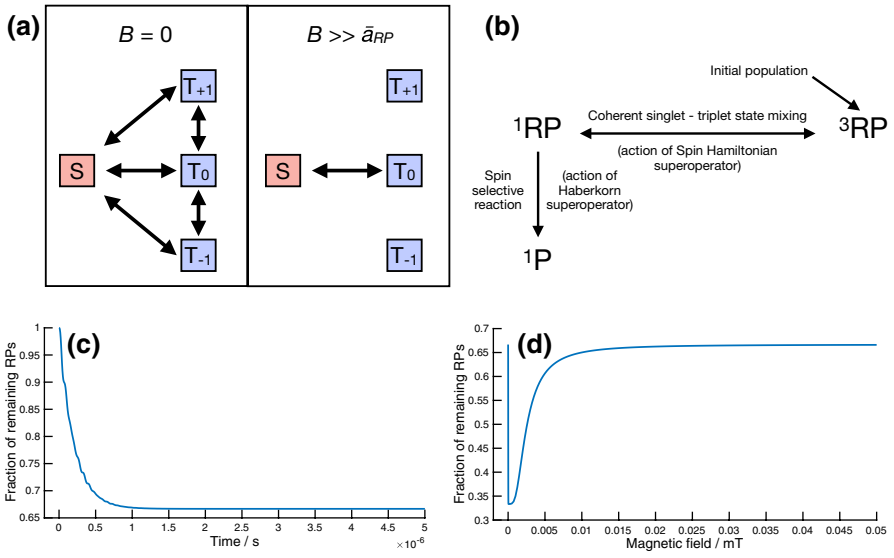

Fig. 1 **a** Common simple model used to represent the changes in singlet-triplet spin-state mixing for a RP in zero and applied field. **b** Simple reaction model used in the simulations in this work. As no relaxation processes are modelled, triplet eigenstates of the RP remain trapped. **c** Time dependence of the RP concentration for a RP with a single spin-1/2 nucleus in a magnetic field of 500 mT. **d** Magnetic field dependence of the RP concentration remaining after 10 microseconds. At zero field [RP] = 1/3, at 0.1 mT, [RP] = 2/3 and at 50 mT, [RP]=1/3

of a magnetic field, the T_{+1} state is raised and the T_{-1} state lowered in energy relative to the S and T_0 states through the Zeeman interaction. When this energy separation becomes large relative to the hyperfine couplings in the RP that drive $S - T$ mixing, then the T_{+1} and T_{-1} states become isolated and so coherent $S - T_{+1}$ and $S - T_{-1}$ mixing becomes impossible. What this means is that for a singlet born RP, two thirds of the possible triplet states are inaccessible, and only mixing with the $[T_0]$ states is possible. For a (non-polarised) triplet born radical pair, two-thirds of the RPs are born in states ($[T_{+1}]$ and $[T_{-1}]$) that are completely incapable of undergoing mixing to the singlet state and so remain trapped in the triplet state.

Based on this simple model, we can undertake a thought experiment. Let us imagine a (not realistic) scenario in which a RP ensemble is born in the triplet state and undergoes coherent spin-state mixing. We allow singlet pairs to react while triplet pairs undergo no reaction. We then wait until the reaction is complete and the system undergoes no further change. According to the simple RP reaction model, if this process is performed in a sufficiently strong magnetic field, at the end of the reaction, we would expect to find one third of our initial ensemble as singlet state products and two thirds of our ensemble still as unreacted radical pairs—half in the T_{+1} state and half in the T_{-1} state. For the zero field case, following the simple model, we might expect to find all the initial ensemble as singlet state product. We will see that this is not actually the case, but the existing model carries this implication. It is, however, a very simple and intuitive way of thinking about how the RPM leads to magnetic field effects, especially for non-specialists and can be used in simple kinetic treatments of reactions proceeding through RPs.

In reality, it is also well known that the real picture is not this simple. In particular, there is an additional effect, known as the low field effect (LFE), which explains that the efficiency of singlet–triplet mixing is not optimal in zero field and can increase with the application of a very weak magnetic field. It is this phenomenon which is believed to be responsible for the magnetosensitivity of plants and animals to the geomagnetic field. Brocklehurst and McLauchlan [12] explained this effect based on the conservation of spin angular momentum, while the precise mechanism was corrected and detailed with great clarity recently by Lewis et al. [13]. In view of this, one can ask the simple question of whether our earlier prediction for the result of the thought experiment in zero field is correct or not, and what the result would be in a weak field where the maximum LFE is observed. Put another way, do zero and weak magnetic field conditions simply deplete the RP population and increase the singlet product populations at different rates, or are some triplet states unable to go undergo mixing to the singlet state, remaining trapped as triplet RPs, as is seen at higher fields due to the Zeeman effect?

To answer this question, the simplest approach is to perform the thought experiment directly, by simulating the spin dynamics using the standard Liouville space density matrix approach. We create a density matrix containing two blocks, one which represents the RP state and the other the singlet product. We begin by populating only the RP state with a density matrix representing an even mixture of T_{+1}, T_0 and T_{-1} states. The density matrix then evolves according to the Liouville von Neumann equation.

$$i\hbar\frac{\partial\rho(t)}{\partial t} = [\hat{H}, \rho(t)] + \{\hat{K}, \rho(t)\} \tag{1}$$

This consists of a commutator constructed from the spin-Hamiltonian operator describing coherent spin-state mixing in the RP driven by the electron-nuclear hyperfine interaction and the electron Zeeman effect, and an anticommutator constructed from the Haberkorn operator [14] which is set up to allow reaction only from singlet RPs with a rate coefficient, k_S and which transfers population from the RP block to the singlet product block. The code written to perform the simulations used functions from the Spinach [15] codebase.

$$\hat{H} = \hat{H}_{\text{Zeeman}} + \hat{H}_{\text{hyperfine}} \tag{2}$$

$$= \mu_B B(g_e\hat{S}_{1z} + g_e\hat{S}_{2z}) + \sum_i a_i\hat{S}_1 \cdot \hat{I}_{1i} + \sum_j a_i\hat{S}_2 \cdot \hat{I}_{2j} \tag{3}$$

$$\hat{K} = \frac{k_S}{2}\hat{P}_S \tag{4}$$

No electron–electron exchange or dipolar interactions are included and the g values of both radicals in the pair are set equal for clarity. No relaxation term is included and so any triplet states that cannot undergo coherent singlet-triplet mixing remain trapped in the RP state. Figure 1b shows the reaction scheme described by the simulations.

Figure 1c shows the time dependence of the RP and singlet product state populations for a RP with a single spin-1/2 nucleus on radical 2, with a hyperfine coupling of (1 mT) in a magnetic field of 500 mT. At this field, the T_{+1} and T_{-1} states are completely isolated energetically from the S and T_0 states and as predicted, the final distribution is two thirds RP and one third singlet product. Table 1a shows the RP density matrix at the end of the reaction [the initial density matrix has values of 1/6 along the main diagonal for all 6 triplet states and 0 for the 2 singlet states (positions 3, 3 and 4, 4)] and illustrates clearly that both T_{+1} states and both T_{-1} states are the ones that remain and that both initially T_0 states have reacted.

Figure 1d shows the magnetic field dependence of the final RP population when the reaction is complete. It is apparent that under no magnetic field conditions do all the triplet born RPs react. In this particular case, at zero field, 2/3 of the population remains in the triplet state and most efficient reaction occurs at around 0.1 mT at which 1/3 of the population remains unreacted, which is a direct observation of the LFE. Let us now explain these observations. To do so, we begin by considering the spin eigenstates of this RP in zero field. These have been presented before by Timmel et al. [16] and in any arbitrary field by Lewis et al. [13] much more recently. Following the state ordering of the latter, the eigenstates in zero field can be written in the singlet-triplet basis as follows:

$$|1\rangle = |T_{+1}\alpha_{2n}\rangle \tag{5}$$

Table 1 Density matrices presented in the singlet–triplet basis at the end of the spin-dynamic simulations for the single spin-1/2 nucleus RP with hyperfine coupling of 1 mT in (a) a 500 mT field, (b) a 0.5 mT field and (c) zero field

(a)	$\|T+{}_1\alpha_{2n}>$	$\|T+{}_1\beta_{2n}>$	$\|S\alpha_{2n}>$	$\|S\beta_{2n}>$	$\|T_0\alpha_{2n}>$	$\|T_0\beta_{2n}>$	$\|T-{}_1\alpha_{2n}>$	$\|T-{}_1\beta_{2n}>$
$\|T+{}_1\alpha_{2n}>$	0.16667	0	0	0	0	0	0	0
$\|T+{}_1\beta_{2n}>$	0	0.16667	0	0	0	0	0	0
$\|S\alpha_{2n}>$	0	0	0	0	0	0	0	0
$\|S\beta_{2n}>$	0	0	0	0	0	0	0	0
$\|T_0\alpha_{2n}>$	0	0	0	0	0	0	0	0
$\|T_0\beta_{2n}>$	0	0	0	0	0	0	0	0
$\|T-{}_1\alpha_{2n}>$	0	0	0	0	0	0	0.16667	0
$\|T-{}_1\beta_{2n}>$	0	0	0	0	0	0	0	0.16667
(b)	$\|T+{}_1\alpha_{2n}>$	$\|T+{}_1\beta_{2n}>$	$\|S\alpha_{2n}>$	$\|S\beta_{2n}>$	$\|T_o\alpha_{2n}>$	$\|T_o\beta_{2n}>$	$\|T-{}_1\alpha_{2n}>$	$\|T-{}_1\beta_{2n}>$
$\|T+{}_1\alpha_{2n}>$	0.16667	0	0	0	0	0	0	0
$\|T+{}_1\beta_{2n}>$	0	0	0	0	0	0	0	0
$\|S\alpha_{2n}>$	0	0	0	0	0	0	0	0
$\|S\beta_{2n}>$	0	0	0	0	0	0	0	0
$\|T_0\alpha_{2n}>$	0	0	0	0	0	0	0	0
$\|T_0\beta_{2n}>$	0	0	0	0	0	0	0	0
$\|T-{}_1\alpha_{2n}>$	0	0	0	0	0	0	0	0
$\|T-{}_1\beta_{2n}>$	0	0	0	0	0	0	0	0.16667
(c)	$\|T+{}_1\alpha_{2n}>$	$\|T+{}_1\beta_{2n}>$	$\|S\alpha_{2n}>$	$\|S\beta_{2n}>$	$\|T_o\alpha_{2n}>$	$\|T_o\beta_{2n}>$	$\|T-{}_1\alpha_{2n}>$	$\|T-{}_1\beta_{2n}>$
$\|T+{}_1\alpha_{2n}>$	0.16667	0	0	0	0	0	0	0
$\|T+{}_1\beta_{2n}>$	0	0.05556	0	0	0.07857	0	0	0
$\|S\alpha_{2n}>$	0	0	0	0	0	0	0	0
$\|S\beta_{2n}>$	0	0	0	0	0	0	0	0
$\|T_0\alpha_{2n}>$	0	0.07857	0	0	0.11111	0	0	0
$\|T_0\beta_{2n}>$	0	0	0	0	0	0.11111	0.07857	0
$\|T-{}_1\alpha_{2n}>$	0	0	0	0	0	0.07857	0.05556	0
$\|T-{}_1\beta_{2n}>$	0	0	0	0	0	0	0	0.16667

$$|2\rangle = \frac{1}{\sqrt{2}}(|T_0\alpha_{2n}\rangle + |S\alpha_{2n}\rangle) \tag{6}$$

$$|3\rangle = \frac{1}{2}(|T_0\alpha_{2n}\rangle - |S\alpha_{2n}\rangle) + \frac{1}{\sqrt{2}}|T_{+1}\beta_{2n}\rangle \tag{7}$$

$$|4\rangle = \frac{1}{2}(|T_0\alpha_{2n}\rangle - |S\alpha_{2n}\rangle) - \frac{1}{\sqrt{2}}|T_{+1}\beta_{2n}\rangle \tag{8}$$

$$|5\rangle = \frac{1}{2}(|T_0\beta_{2n}\rangle + |S\beta_{2n}\rangle) - \frac{1}{\sqrt{2}}|T_{-1}\alpha_{2n}\rangle \tag{9}$$

$$|6\rangle = \frac{1}{2}(|T_0\beta_{2n}\rangle + |S\beta_{2n}\rangle) + \frac{1}{\sqrt{2}}|T_{-1}\alpha_{2n}\rangle \tag{10}$$

$$|7\rangle = \frac{1}{\sqrt{2}}(|T_0\beta_{2n}\rangle - |S\beta_{2n}\rangle) \tag{11}$$

$$|8\rangle = |T_{-1}\beta_{2n}\rangle \tag{12}$$

where α_{2n} indicates a nuclear spin in the alpha state attached to radical 2. These states are quite difficult to visualise and their form can easily cloud the rather straightforward changes in spin-state that define them. To shed a little more light on their interpretation, we take a step back and try to generate them intuitively. To do so, we consider the simplest possible representation of the eight states of a RP in the product basis.

$$|P1\rangle = |\alpha_{1e}\alpha_{2e}\alpha_{2n}\rangle \tag{13}$$

$$|P2\rangle = |\alpha_{1e}\alpha_{2e}\beta_{2n}\rangle \tag{14}$$

$$|P3\rangle = |\alpha_{1e}\beta_{2e}\alpha_{2n}\rangle \tag{15}$$

$$|P4\rangle = |\alpha_{1e}\beta_{2e}\beta_{2n}\rangle \tag{16}$$

$$|P5\rangle = |\beta_{1e}\alpha_{2e}\alpha_{2n}\rangle \tag{17}$$

$$|P6\rangle = |\beta_{1e}\alpha_{2e}\beta_{2n}\rangle \tag{18}$$

$$|P7\rangle = |\beta_{1e}\beta_{2e}\alpha_{2n}\rangle \tag{19}$$

$$|P8\rangle = |\beta_{1e}\beta_{2e}\beta_{2n}\rangle \tag{20}$$

4 of these 8 states are not eigenstates of the zero field Spin Hamiltonian. Electron spin 2 and nuclear spin 2 are capable of a simultaneous spin flip, driven by their hyperfine interaction, which serves to interconvert states $|P2\rangle$ and $|P3\rangle$ and states $|P6\rangle$ and $|P7\rangle$. This is the only spin-state mixing process that can take place in zero field. Therefore, the eigenstates of the zero field Hamiltonian can be written by taking linear combinations of these pairs of states. The following states should thus be the zero-field eigenstates.

$$|P1\rangle = |\alpha_{1e}\alpha_{2e}\alpha_{2n}\rangle \tag{21}$$

$$\frac{1}{\sqrt{2}}(|P3\rangle - |P2\rangle) = \frac{1}{\sqrt{2}}(|\alpha_{1e}\beta_{2e}\alpha_{2n}\rangle - |\alpha_{1e}\alpha_{2e}\beta_{2n}\rangle) \tag{22}$$

$$\frac{1}{\sqrt{2}}(|P3\rangle + |P2\rangle) = \frac{1}{\sqrt{2}}(|\alpha_{1e}\beta_{2e}\alpha_{2n}\rangle + |\alpha_{1e}\alpha_{2e}\beta_{2n}\rangle) \tag{23}$$

$$|P4\rangle = |\alpha_{1e}\beta_{2e}\beta_{1n}\rangle \tag{24}$$

$$|P5\rangle = |\beta_{1e}\alpha_{2e}\alpha_{1n}\rangle \tag{25}$$

$$\frac{1}{\sqrt{2}}(|P7\rangle - |P6\rangle) = \frac{1}{\sqrt{2}}(|\beta_{1e}\beta_{2e}\alpha_{2n}\rangle - |\beta_{1e}\alpha_{2e}\beta_{2n}\rangle) \tag{26}$$

$$\frac{1}{\sqrt{2}}(|P7\rangle + |P6\rangle) = \frac{1}{\sqrt{2}}(|\beta_{1e}\beta_{2e}\alpha_{2n}\rangle + |\beta_{1e}\alpha_{2e}\beta_{2n}\rangle) \tag{27}$$

$$|P8\rangle = |\beta_{1e}\beta_{2e}\beta_{1n}\rangle \tag{28}$$

These look very simple but are actually exactly the same states as those presented earlier, which we can demonstrate by rewriting them in the singlet-triplet basis. This is simple using the substitutions for the electron spins:

$$|S\rangle = \frac{1}{\sqrt{2}}(|\alpha_{1e}\beta_{2e}\rangle - |\beta_{1e}\alpha_{2e}\rangle) \tag{29}$$

$$|T_0\rangle = \frac{1}{\sqrt{2}}(|\alpha_{1e}\beta_{2e}\rangle + |\beta_{1e}\alpha_{2e}\rangle) \tag{30}$$

$$|T_{+1}\rangle = |\alpha_{1e}\alpha_{2e}\rangle \tag{31}$$

$$|T_{-1}\rangle = |\beta_{1e}\beta_{2e}\rangle \tag{32}$$

Which produces the states:

$$|P1\rangle = |1\rangle \tag{33}$$

$$\frac{1}{\sqrt{2}}(|P3\rangle - |P2\rangle) = |4\rangle \tag{34}$$

$$\frac{1}{\sqrt{2}}(|P3\rangle + |P2\rangle) = |3\rangle \tag{35}$$

$$|P4\rangle = |7\rangle \tag{36}$$

$$|P5\rangle = |2\rangle \tag{37}$$

$$\frac{1}{\sqrt{2}}(|P7\rangle - |P6\rangle) = |5\rangle \tag{38}$$

$$\frac{1}{\sqrt{2}}(|P7\rangle + |P6\rangle) = |6\rangle \tag{39}$$

$$|P8\rangle = |8\rangle \tag{40}$$

Here the states are identified with the corresponding labels prepared earlier. Clearly, the product basis description makes the spin-state mixing processes transparent while the singlet-triplet basis representation, while hard to visualise, is necessary to understand how the simultaneous nuclear and electron spin flips influence the singlet-triplet character of the pair.

Let us consider first states $|1\rangle$ and $|8\rangle$. These states are the so-called 'end states.' The end states are always the two states with all electron and nuclear spins parallel, and are thus located at either end of the distribution. This means that while they constitute one quarter of the states for a RP with a single spin-1/2 nucleus, they become less and less important for RPs with more spin-active nuclei. They have different m_J from all other states and each other (here + 3/2 and − 3/2 respectively). As conservation of angular momentum always requires the conservation of m_J, these two states can never undergo coherent spin-state mixing and are thus always eigenstates of the spin Hamiltonian under any magnetic field conditions. On this basis, we can understand why the most efficient reaction leads to a final RP population of 1/3, as the two end states can never undergo singlet–triplet state mixing and always remain as triplet RPs. We can confirm that this is the case by examining the RP density matrix at the end of the simulation, corresponding to the peak of the LFE (Table 1b). The only populated states of the RP are indeed these states. This is a very old result and we only reconfirm it here. However, the result is not the same at zero field, which implies that there must be additional triplet eigenstates of this RP when the field is removed. Their identities are not readily apparent when examining states $|2\rangle$ to $|7\rangle$, however.

In their paper, Lewis et al., revisited the original hypothesis made by Brocklehurst and McLauchlan that in zero field, conservation of angular momentum requires that J and m_J are both conserved, while the presence of a field removes the restriction on J, but keeps the restriction on m_J. Brocklehurst and McLauchlan believed that the removal of this restriction allowed mixing from S ($J = 1/2$) to T_{+1} and T_{-1} ($J = 3/2$)

to be unlocked. Lewis et al. identified that this is not correct and demonstrated that it is actually mixing between S and T_0 states that is unlocked when a small field is applied. An unfortunate consequence of this is the loss of the intuitive vector picture describing spin motion in zero and weak field that Brocklehurst and McLauchlan presented. In identifying the additional zero field triplet eigenstates, we will also aim to correct and update this model.

States $|1\rangle, |2\rangle, |3\rangle, |6\rangle, |7\rangle$ and $|8\rangle$ form a degenerate group in zero field ($E = +a/4$) and states $|4\rangle$ and $|5\rangle$ another degenerate group ($E = -3a/4$). To proceed, we take advantage of the fact that for degenerate states, linear combinations of those states are also eigenstates. Taking linear combinations of states 2 and 3 and also of states 6 and 7 as follows, produces a new representation of these eigenstates:

$$|9\rangle = \frac{1}{\sqrt{2}}(|2\rangle) - |3\rangle = |S\alpha_{2n}\rangle - \frac{1}{\sqrt{2}}|T_{+1}\beta_{2n}\rangle \tag{41}$$

$$|10\rangle = \frac{1}{\sqrt{2}}(|2\rangle) + |3\rangle = |T_0\alpha_{2n}\rangle + \frac{1}{\sqrt{2}}|T_{+1}\beta_{2n}\rangle \tag{42}$$

$$|11\rangle = |6\rangle) - \frac{1}{\sqrt{2}}(|7\rangle) = |S\beta_{2n}\rangle + \frac{1}{\sqrt{2}}|T_{-1}\alpha_{2n}\rangle \tag{43}$$

$$|12\rangle = |6\rangle + \frac{1}{\sqrt{2}}(|7\rangle) = |T_0\beta_{2n}\rangle + \frac{1}{\sqrt{2}}|T_{-1}\alpha_{2n}\rangle \tag{44}$$

The result of the simulations in zero field can now be explained. States 10 and 12 are eigenstates of the zero-field Spin Hamiltonian but are also pure triplet states—coherent superpositions of T_{+1} / T_{-1} and T_0. This means that they cannot undergo spin-state mixing and so are trapped as RPs in the zero field simulation. If we examine the RP density matrix remaining at the end of this simulation (Table 1c), it is easy to identify that it is composed of a mixture of the end states ($|1\rangle, |8\rangle$) and the 'new' triplet states ($|10\rangle, |12\rangle$).

It remains the case that mixing between these pairs of states (now $|9\rangle$, $|10\rangle$ and $|11\rangle, |12\rangle$) is not possible due to their degeneracy, and that this degeneracy is lifted with the application of a weak magnetic field. This provides a clear intuition about how the removal of this restriction leads to $S - T_0$ mixing. Mixing between states 9 and 10 and between 11 and 12 is transparently an $S - T_0$ mixing process (the T_{+1} or T_{-1} component is unchanged), while this was far from clear upon examining the original eigenstates that became mixed when a field was applied (2, 3 and 6, 7). It is worth noting that in the vector model picture of $S - T_0$ mixing applied at high field, this mixing occurs, because the individual electron spins go in and out of phase with one another due to the difference in their Larmor frequencies. Clearly, in zero field, the states are degenerate and so such dephasing/rephasing is not possible. We can now rescue Brocklehurst and McLauchlan's vector picture, which was correct in almost all aspects. In zero field, the electron

spin and nuclear spin of radical two precess around their resultant. When considered along with the electron spin of radical 1, this process corresponds to coherent mixing between $S\alpha_{2n}$ and $T_{+1}\beta_{2n}$ (in the case of state 9) as shown in Fig. 2a. Applying a weak magnetic field causes this resultant to precess around the field direction, which corresponds to $S - T_0$ mixing. The vector model provides a very

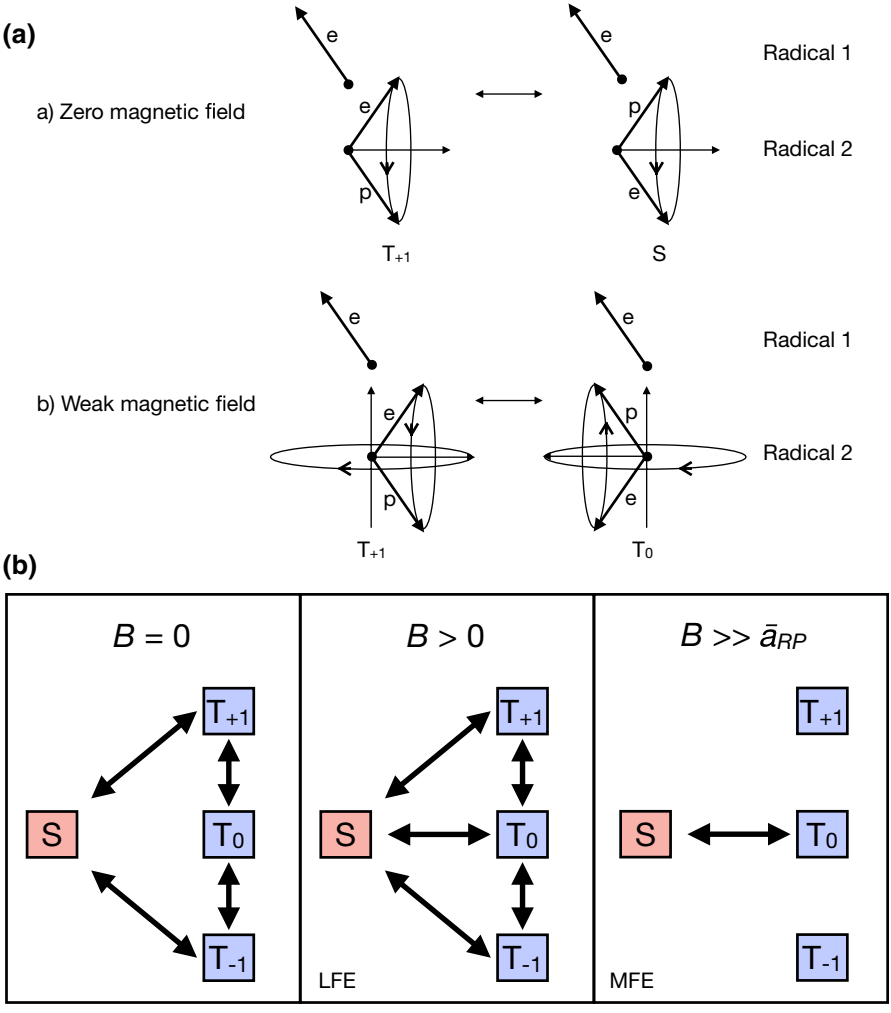

Fig. 2 **a** Vector model for spin-state mixing in zero and weak magnetic fields. This is an updated and corrected version of that given by Brocklehusrt and McLauchlan [12]. In zero field, precession about the resultant magnetic moment of the electron and nuclear spins on radical 2 causes the electron spin of the pair to oscillate between S and T_{+1} states (an equivalent picture can be drawn for the oscillation between S and T_{-1} with the opposite electron spin). When a weak magnetic field is applied, the resultant begins to precess about the field direction and so the horizontal precession causes $S - T_0$ mixing, while the vertical precession now corresponds to both $S - T_{+1}$ and $T_0 - T_{+1}$ mixing. **b** An update to the simple picture in Fig. 1a which correctly identifies the possible spin mixing pathways in zero, weak and strong (much greater than the average hyperfine coupling of the RP ($\bar{a}_{RP}$))

effective picture of what happens when the degeneracies of states $|9\rangle, |10\rangle$ and $|11\rangle, |12\rangle$ are lifted.

Figure 2a also allows us to achieve an intuitive understanding of why half of the T_{+1} / T_{-1} states only mix with T_0 and the other half mix with S. There is always a phase relationship between the two electron spins, which is consequential in the case of S and T_0 (indeed, it defines the difference between them) and initially appears inconsequential in the case of T_{+1} and T_{-1}. However, the phase difference in the latter two states is clearly not inconsequential, but indeed defines whether the result of a nuclear spin–electron spin flip-flop transition results in a S or T_0 state—i.e. the phase difference is preserved in the T_{+1} / T_{-1} states (for intuition, we can imagine that when both electron spins are on the same side of the precession cone in (for example) T_{+1}, the result is T_0, while it is S when they are on the same side).

In summary, at zero field, coherent singlet-triplet state mixing only occurs through simultaneous flipping of hyperfine coupled electron and nuclear spins, while in high field it only occurs through the electron spin dephasing/rephasing due to differences in the rate of precession about the applied field. The LFE exists because both mechanisms are possible in weak magnetic fields. With this understanding, and the identification of the zero field triplet eigenstates, it is now possible to 'update' the simple kinetic representation of magnetic field effects as well, which is presented in Fig. 2b. It is hoped that this intuitive picture, which is not strictly correct (end-states are ignored), but captures the results of the key spin dynamics, will prove useful to non-specialists in need of a simple picture of the origin of the regular MFE and the LFE.

Finally, for states with increasing numbers of spin-active nuclei, the number of end states remains fixed at two, and so the size of the spin-space capable of singlet-triplet mixing grows. It is useful to consider the number of (non end-state) zero-field triplet eigenstates as the number of spin-active nuclei increases. These are easily determined by performing the simulation in zero field for an increasing number of coupled nuclei. Such simulations demonstrate that the number of zero-field triplet eigenstates in the case of non-degenerate spin-1/2 nuclei is equal to the number of nuclear spins+1. This means that the fraction of zero-field triplet eigenstates drops rapidly as the number of nuclear spins increases, because the total eigenstate count increases by a factor of 2 with each additional spin-1/2 nucleus, while the zero-field triplet eigenstate count increases by only 1.

For example, in the case of a single spin-1/2 nucleus considered here, of the 8 eigenstates, the zero field triplet eigenstate count is 2—i.e. one quarter of all states. For two spin-1/2 nuclei, there are only 3 zero-field triplet eigenstates from a total of 16. For three spin-1/2 nuclei, the fraction has already dropped to 4 in 32. The reasons for and implications of this phenomenon for the LFE in more realistic systems along with the case for nuclei with spin $> 1/2$ will be presented in a future article. For the purposes of the overarching mechanism considered here, it is worth highlighting that none of the additional singlet-triplet mixing pathways available in larger spin systems arise from $S - T_0$ mixing, but simply much more efficient $S - T_{\pm 1}$ mixing, so the models presented hold in such systems. In addition, it is clear that the maximum magnitude of the LFE drops rapidly with the number of hyperfine coupled nuclei, which is significant for the structure of a molecular magnetic compass optimised for sensing weak magnetic fields.

3 Conclusions

Through simple density matrix RP spin dynamic simulations with no triplet reaction channel, we have identified that there are zero-field triplet states of RPs that cannot undergo coherent spin state mixing. We have demonstrated that these states can readily be derived by taking suitable linear combinations of the known zero-field eigenstates and that the form of these linear combinations also reveal why a lifting of their degeneracies results in $S - T_0$ mixing. Using these observations, we have constructed two different, simple visual representations of the low field effect, which we hope will make the LFE mechanism accessible to a much wider audience.

Author Contributions J. R. Woodward did all research and wrote the manuscript.

Funding This work was supported by the Japan Society for the Promotion of Science (JSPS) Grants-in-Aid for Scientific Research (Grant number 20H02687).

Code Availability The code used for the simulations described in this work is available from the corresponding author on reasonable request.

Declarations

Conflict of Interest The authors declare no competing interests.

References

1. G. Closs, J. Am. Chem. Soc. **91**(16), 4552–4554 (1969)
2. R. Kaptein, J. Oosterhoff, Chem. Phys. Letts. **4**, 195 (1969)
3. R. Kaptein, J. Oosterhoff, Chem. Phys. Lett. **4**, 214–216 (1969)
4. R.W. Fessenden, R.H. Schuler, J. Chem. Phys. **39**(9), 2147–2195 (1963)
5. J. Bargon, H.F., Johnsen, U. Naturforsch. 22, 1551–1555 (1967)
6. J. Bargon, H.F., Johnsen, U. Naturforsch. 22, 1556–1560 (1967)
7. H.R. Ward, R.G. Lawler, J. Am. Chem. Soc. **89**, 5518–5519 (1967)
8. R. Sagdeev, Y. Molin, K. Salikhov, T. Leshina, M. Kamha, S. Shein, Org. Magn. Reson. Soc. **5**, 603–605 (1973)
9. B. Brocklehurst, R.S. Dixon, E. Gardy, V. Lopata, M. Quinn, A. Singh, F. Sargent, Chem. Phys. Lett. **28**, 361–363 (1974)
10. K. Maeda, K.B. Henbest, F. Cintolesi, I. Kuprov, D.T. Rodgers, P.A. Liddell, D. Gust, C.R. Timmel, P.J. Hore, Nature **453**, 387–390 (2008)
11. P.W. Atkins, G.T. Evans, Chem. Phys. Lett. **25**(1), 108–110 (1974)
12. B. Brocklehurst, K.A. McLauchlan, Int. J. Radiat. Biol. **69**(1), 3–24 (1995)
13. A.M. Lewis, T.P. Fay, D.E. Manolopoulos, C. Kerpal, S. Richert, C.R. Timmel, J. Chem. Phys. **149**, 034103 (2018)
14. R. Haberkorn, Mol. Phys. **32**(5), 1491–1493 (1976)
15. H.J. Hogben, M. Krzystyniak, G.T.P. Charnock, P.J. Hore, I.J. Kuprov, Mag. Reson. **208**, 179–194 (2012)
16. C.R. Timmel, P.J. Hore, Chem. Phys. Lett. **257**, 40–408 (1996)